the formation of CdTe. Thus, free Te^0 phase formation is precluded in the anodic pathway. On the other hand, in the cathodic route, *Te^0 nucleation precedes and is a requirement for CdTe formation.*[42] Thus Te^0 contamination is a common occurrence with cathodic CdTe thin-film growth.[24]

Figure 8 shows the results of a XPS survey scan (Figure 8a) and high-resolution scans for Cd (Figure 8b) and Te (Figure 8c). Integration of the high-resolution XPS peaks yielded elemental concentrations similar to those given by the Auger measurements: Cd, 31.0%; Te, 32.5%; C, 23.4%; O, 12.9%. The peak positions (charge referenced to the C 1s peak, which was taken to be 284.6 eV) indicate binding energies of 411.4 and 404.6 eV for the Cd $3d_{3/2}$ and $3d_{5/2}$ peaks and 582.4 and 572 eV for the Te $3d_{3/2}$ and the Te $3d_{5/2}$ peaks, respectively. These binding energies are within 0.1 eV of values for single-crystal CdTe reported by Kibel and Kelly[43] and are in reasonable agreement with other previously reported values.[44] Further, the peak shapes and binding energies in Figure 8c rule out the presence of significant amounts of Te oxides, which if present would have produced an easily resolved peak 3.7 eV higher in binding energy than the observed position.[43,44] Thus, we attribute the nonsurface O to the presence of $CdO/Cd(OH)_2$ in minor quantities in addition to CdTe as the major component.

In conclusion, we have demonstrated that CdTe thin films with little contamination from Te^0 may be electrosynthesized via an anodic route. A anodic electroless technique was also used for the first time to electrosynthesize n-type CdTe thin films.

Acknowledgment. We thank the National Science Foundation (Grant MSM 86-17850) for partial financial support of this research. It is also a pleasure to acknowledge the support of the Research Enhancement Program of The University of Texas at Arlington. A.W. additionally thanks the Robert A. Welch Foundation and the Texas Advanced Research Program for funding support. M. Murley of LTV, Dallas, TX, provided the surface analysis data.

Registry No. CdTe, 1306-25-8; Cd, 7440-43-9; Na_2Te, 12034-41-2; Te^{2-}, 22541-49-7; Te_2^{2-}, 62086-49-1; Kr, 7439-90-9.

(42) Mori, E.; Rajeshwar, K. *J. Electroanal. Chem.* **1989**, *258*, 415.
(43) Kibel, M. H.; Kelly, C. G. *Mater. Australasia* **1987**, *Nov/Dec*, 15.
(44) Briggs, D.; Seah, M. P. *Practical Surface Analysis*; Wiley: Chichester, UK, 1982.

A Surface Characterization and Depth Profiling Study of Conventional Electrodeposited Chromium Films. 3

Gar B. Hoflund,* Mark R. Davidson, and Eva Yngvadottir

Department of Chemical Engineering, University of Florida, Gainesville, Florida 32611

Herbert A. Laitinen

Department of Chemistry, University of Florida, Gainesville, Florida 32611

Shigeo Hoshino

Musashi Institute of Technology, 1-28, Tamazutsumi, Setagaya-ku, Tokyo 158, Japan

Received April 20, 1989

In this study the composition and chemical interactions of chromium layers produced in a conventional Sargent bath have been examined using Auger electron spectroscopy (AES), electron spectroscopy for chemical analysis (ESCA), ion scattering spectroscopy (ISS), and depth profiling before and after annealing the sample in air or vacuum. Future comparisons between these results and similar results obtained from chromium layers prepared by the amorphous bright chromium deposition (ABCD) method (Hoshino, S.; Laitinen, H. A.; Hoflund, G. B. *J. Electrochem. Soc.* **1986**, *133*, 681) should be useful in understanding why the ABCD films behave differently than conventional Cr films. ABCD films have many desirable properties compared to deposits produced by conventional methods. Most importantly, the hardness of ABCD films increases with annealing temperature up to 700 °C, whereas the hardness of conventional chromium films decreases. The results of this study indicate that S, C, Cl, O, Ca, K, and Na are incorporated into the conventional chromium films from the electrolytic bath. Cr is present as a sulfide, metal, and oxides. Annealing the sample in air or vacuum (10^{-4} Torr) causes sulfur to desorb from the surface probably as SO_2. Annealing the sample in high vacuum (5×10^{-9} Torr) causes sulfur to segregate to the surface and remain there while oxygen migrates to the surface and desorbs. This results in conversion of the surface chromium oxides into Cr_2S_3 and metallic Cr. Carbon present in the background gas during annealing is adsorbed and incorporated into the bulk of the film.

Introduction

Chromium plating is widely used in the manufacture of machines and instruments in the automobile and other industries to improve the wear resistance of metallic surfaces and protect them against corrosion. Sargent[1] and Fink[2] developed and described methods that use chromic acid solutions containing a sulfate catalyst for chromium plating. The chromium plating layers formed by this method have many defects, which may be described as crack and pinhole defects. Also, the hardness of these

(1) Sargent, G. J. *Trans. Am. Electrochem. Soc.* **1920**, *37*, 479.
(2) Fink, C. G. U.S. Patent 1,581,188, 1926.

0897-4756/89/2801-0625$01.50/0

deposits decreases with increasing annealing temperature. A trivalent chromium bath has been developed by Crowther and Renton,[3] but this bath can be used only for decorative chromium platings because the layers are thin. These chromium deposits show an amorphous structure according to X-ray diffraction measurements. Amorphous chromium deposits have been discussed by Furuya et al.[4] and Morikawa and Eguchi.[5] They obtained amorphous chromium deposits from chromic acid solutions containing trivalent chromium ions and large quantities of organic compounds. They also found it difficult to deposit thick chromium layers in these baths.

Hoshino et al.[6] have developed a method for preparing amorphous, bright chromium films from chromic acid solutions containing organic compounds that have a CHO or COOH group such as formic acid, formaldehyde, formamide, or glyoxal. This method is referred to as the amorphous, bright chromium deposition (ABCD) method. The initial Vicker's hardness of these films is 1000 and goes through a maximum of about 1700 between 500 and 600 °C for an annealing time of 30 min. This is not the case for the conventional chromium films, which have an initial hardness of about 800; but this hardness decreases to almost 400 as the annealing temperature increases to 800 °C. This decrease in hardness severely limits the usefulness of conventional Cr films in high-temperature applications. Compared to conventional Cr platings, the ABCD films have lower defect densities and are more resistant to corrosion by hydrochloric acid. X-ray diffraction shows that the unannealed ABCD films are amorphous. Annealing at temperatures between 400 and 600 °C causes growth and formation of Cr crystallites while bulk-phase chromium carbides and oxides form above 600 °C. Surface characterization studies of ABCD deposits have been presented by Hoflund and co-workers.[7,8]

The objective of the present study is to determine the composition and chemical states of the species present at surfaces of conventional Cr films before and after various treatments. Future studies will focus on the comparison of the results obtained from ABCD and conventional Cr films to obtain an understanding of the different hardness behavior of conventional and ABCD films as a function of annealing temperature. In this study, Auger electron spectroscopy (AES), electron spectroscopy for chemical analysis (ESCA), ion scattering spectroscopy (ISS), and sputter-depth profiling have been used to examine the surface and bulk regions of conventional Cr platings before and after annealing the sample in air and vacuum at 600 °C.

Experimental Section

The conventional Cr layers were prepared by electrodepositing Cr from a solution containing 250 g/L of chromic acid and 2.5 g/L of sulfuric acid at a temperature of 50 °C and a current density of 40 A/dm^2 for 30 min. After deposition the samples were ultrasonically cleaned in acetone and ethanol.

AES, ESCA, and ISS were performed using a double-pass cylindrical mirror analyzer (CMA, PHI Model 25-270 AR) contained in a vacuum system with a base pressure of 5×10^{-11} Torr.

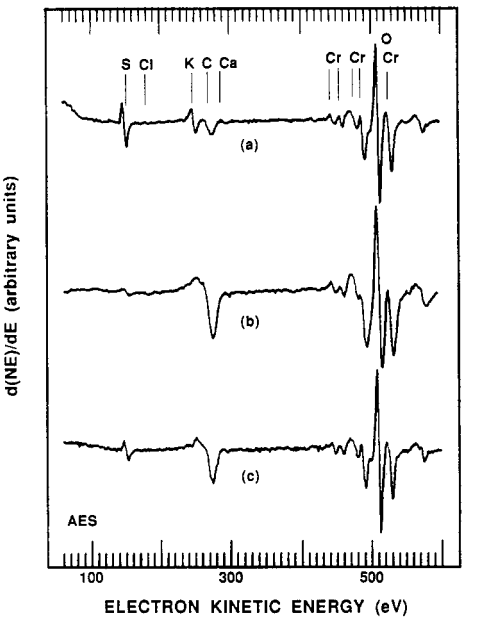

Figure 1. AES spectra taken from conventional Cr samples (a) before annealing or sputtering, (b) after annealing at 600 °C for 30 min in air, and (c) after annealing at 600 °C for 30 min in a 10^{-4}-Torr vacuum.

AES data were obtained by using a primary-beam energy of 3 keV. The CMA was operated in the nonretarding mode with a peak-to-peak oscillation voltage of 0.5 V and a 5-kHz frequency. A 20-μA primary-beam current was focused to a spot approximately 0.5 mm in diameter. ESCA data were taken in the retarding mode with a pass energy of 50 eV using a computer-interfaced, digital, pulse-counting circuit[9] and digital filtering techniques.[10] Utilization of smaller pass energies does not result in significantly increased resolution. Also, the conditions used to collect AES and ESCA spectra result in negligible damage to the surface. ISS was carried out in the nonretarding mode using a defocused primary beam of 1-keV He ions (100 nA over an area 1 cm in diameter for 1 min). The ISS primary beam flux was minimized to minimize beam damage. Primary-beam-induced damage was negligible since ISS spectra taken repeatedly show negligible differences. Ion sputtering was performed using a sputter gun system (PHI Model 04-161) to produce an argon-ion beam of 0.5 keV and 2 μA over a spot diameter of approximately 1 cm. The sample was heated radiantly with a 0.5-mm tungsten filament placed behind the sample, and the temperature of the sample was measured with an optical pyrometer. Charging did not occur in the application of any of these techniques to the various samples examined.

Results and Discussion

Figure 1a shows an AES spectrum taken from the surface of an as-prepared sample. Peaks due to S, Cl, K, C, Ca, O, and Cr are observed. A Na peak, which is not shown, appears at 990 eV. Cl is a trace impurity in the reagent grade salts and acids that are used in the film preparation. It often appears as a surface contaminant in small quantities. Ca, K, and Na are contaminants from the glassware used to store solutions, and S is a component in the electrolytic bath. The C may be a solution contaminant but probably adsorbs during exposure of the film to air. The C peak shape indicates that most of the C is of graphitic form.[11] Although this contaminating C is

(3) Crowther, J. C.; Renton, A. *Electroplat. Met. Finish.* **1975**, *28*, 6.
(4) Furuya, H.; Misaki, Y.; Tanabe, Y. *J. Met. Finish. Soc. Jpn.* **1981**, *32*, 631.
(5) Morikawa, T.; Eguchi, S. presented at the 70th Annual Conference of the Metal Finishing Society of Japan, 1984.
(6) Hoshino, S.; Laitinen, H. A.; Hoflund, G. B. *J. Electrochem. Soc.* **1986**, *133*, 681.
(7) Hoflund, G. B.; Asbury, D. A.; Babb, S. J.; Grogan, A. L., Jr.; Laitinen, H. A.; Hoshino, S. *J. Vac. Sci. Technol. A* **1986**, *4*, 26.
(8) Hoflund, G. B.; Grogan, A. L., Jr.; Asbury, D. A.; Laitinen, A.; Hoshino, S. *Appl. Surf. Sci.* **1987**, *28*, 224.
(9) Gilbert, R. E.; Cox, D. F.; Hoflund, G. B. *Rev. Sci. Instrum.* **1982**, *53*, 1281.
(10) Savitzky, A.; Golay, M. J. E. *Anal. Chem.* **1984**, *36*, 1627.
(11) Davis, L. E.; MacDonald, N. C.; Palmberg, P. W.; Riach, G. E.; Weber, R. E. *Handbook of Auger Electron Spectroscopy*; Physical Electronics Ind.: Eden Prairie, MN, 1976).

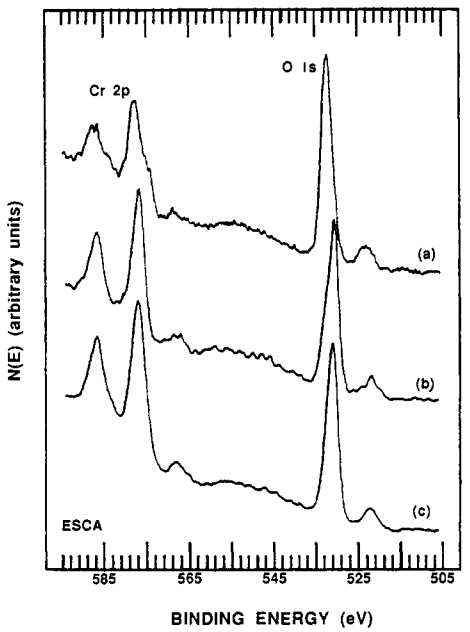

Figure 2. ESCA spectra showing the Cr 2p and O 1s peaks taken (a) from the as-prepared sample, (b) after annealing at 600 °C for 30 min in air, and (c) after annealing at 600 °C for 30 min in a 10^{-4}-Torr vacuum.

Table I. ESCA Peak Energy Assignments[a]

element peak	species	binding energy, eV
oxygen 1s	Cr_2O_3	530.2
	$Cr(CO)_6$	534.3
chromium $2p_{3/2}$	metal	574.0
	CrO_2	576.0
	Cr_2O_3	576.6
	CrO_3	578.0
	CrOOH	576.8
	Cr_2S_3	574.6
	CrN	575.5
	$CrCl_3$	577.5

[a] Most of these assignments are taken from ref 7.

typically referred to as graphitic in surface studies, neither its structure nor composition has been well characterized, and the C-containing phase probably contains both H and O and has an amorphous structure.

Figure 2a shows a Cr 2p and O 1s ESCA spectrum taken from the as-prepared Cr sample. Peak assignments for several Cr and O species are listed in Table I. A more detailed spectrum of the Cr 2p peaks is shown in Figure 3a. The line shape of the Cr $2p_{3/2}$ peak indicates that the Cr is present in more than one oxidation state. The shoulder at 574.2 eV is due to metallic Cr, and the shoulder at 574.8 eV is due to Cr_2S_3. The Cr is also present in oxidic forms: Cr_2O_3 at 576.6 eV, CrO_3 at 578.0 eV, and probably some CrOOH at 576.8 eV. On the basis of the relative peak areas and standard atomic sensitivity factors (0.63 for O and 1.7 for Cr),[12] the O/Cr atomic ratio is about 3.5. Therefore, a significant portion of the O present is not bonded to the Cr as an oxide. Also, the O 1s peak lies at 532.2 eV while the O bonded as Cr_2O_3 would appear at 530.2 eV. A slight nonsymmetrical broadening of the O 1s peak on the low binding energy side (see Figure 4a) is probably due to O bonded as Cr_2O_3. It is possible that most of the O present is in the form of adsorbed water and hydroxyl groups.

(12) Wagner, C. D.; Riggs, W. M.; Davis, L. E.; Moulder, J. F.; Muilenberg, G. E. *Handbook of X-ray Photoelectron Spectroscopy*; Perkin-Elmer: Eden Prairie, MN, 1979).

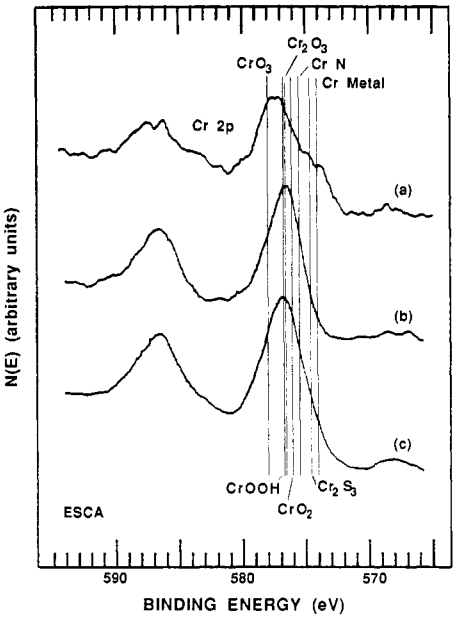

Figure 3. Cr 2p ESCA spectra of Figure 2 shown on an expanded scale.

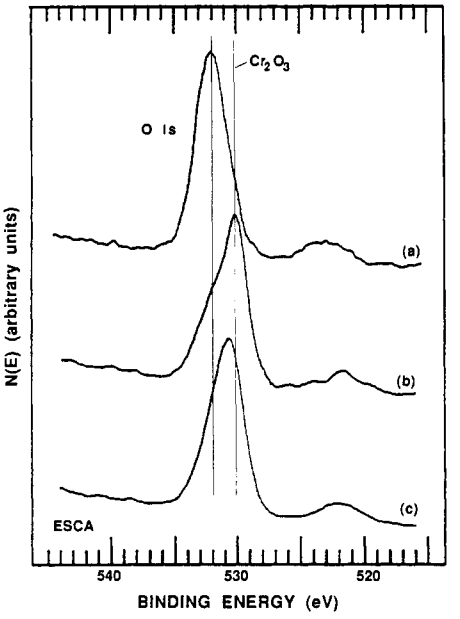

Figure 4. O 1s ESCA spectra of Figure 2 shown on an expanded scale.

An AES spectrum taken after annealing the conventional Cr sample at 600 °C in air for 30 min is shown in Figure 1b. The S and K peaks are greatly decreased while the C peak is greatly increased. This indicates either that annealing the sample in air causes the C to segregate to the surface or that C is adsorbed at the surface during annealing or cooling. This point is discussed further below with regard to the depth profiling results. The shape of the C peak indicates that it is graphitic. The S most likely reacts with O in the air and desorbs as SO_2, and the K probably desorbs as an oxide. It is interesting that annealing an as-prepared sample in air results in a reduction in the O/Cr atomic ratio from 1.7 to 1.5. This is probably due to decomposition of CrO_3 and CrOOH to Cr_2O_3, which is more stable at elevated temperatures. The Ca and Cl peaks seem to remain unchanged.

An ESCA spectrum of the Cr 2p and O 1s peaks after annealing the sample at 600 °C in air is shown in Figure

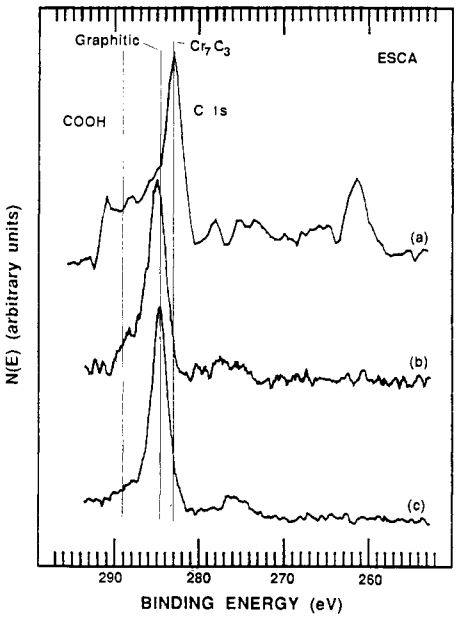

Figure 5. ESCA C 1s spectra taken (a) from the as-prepared sample, (b) after annealing at 600 °C for 30 min in air, and (c) after annealing at 600 °C for 30 min in a 10^{-4}-Torr vacuum.

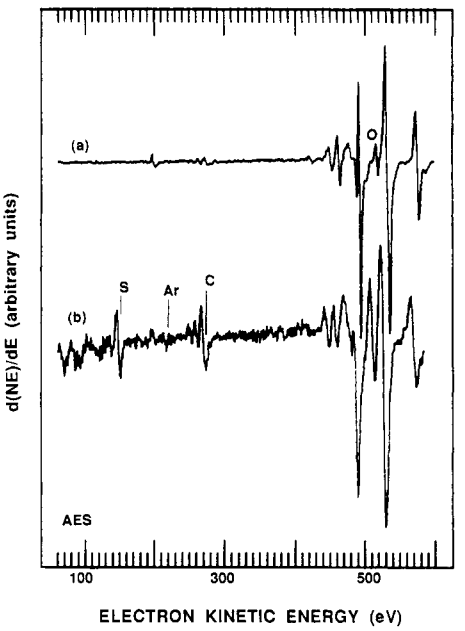

Figure 6. AES spectra taken (a) from the as-prepared sample and (b) of the 10^{-4}-Torr vacuum-annealed sample after ion sputtering both samples for 19 h.

2b. The predominant O 1s peak (see Figure 4b) has an energy of 530.2 eV, which indicates that the O is mostly incorporated as Cr_2O_3. A nonsymmetical broadening of this peak on the high binding energy side (see Figure 4b) is probably due to the presence of O as COOH, hydroxyl groups, or adsorbed water and perhaps a small amount bonded as $Cr(CO)_6$. A more detailed ESCA spectrum of the Cr 2p peaks is shown in Figure 3b. The Cr $2p_{3/2}$ peak shows that the Cr is mostly present in oxidic form as Cr_2O_3. This peak has a slight nonsymmetrical broadening on the high binding energy side which is probably due to CrO_3. Metallic Cr does not appear to be present. According to the ESCA spectra shown in Figure 2, annealing in air reduces the O/Cr atomic ratio from 3.5 to 2.7. Thus, both the AES and ESCA spectra are in agreement that annealing an as-prepared sample in air reduces the O/Cr atomic ratio.

Annealing the conventional Cr sample at 600 °C in a vacuum (mechanically pumped to 10^{-4} Torr) for 30 min causes changes in the spectral features. Figure 1c shows an AES spectrum taken after annealing the sample in vacuum. The S peak is decreased while the C peak is increased. The shape of the C peak indicates that most of the C is of graphitic form. The K is almost completely desorbed from the surface, and the Cl, Ca, and O peaks seem unchanged. These changes are similar to those observed after annealing in air in that the S peak is reduced and the C peak is increased. Also, the O/Cr atomic ratio apparently does not change. This sample was exposed to air after the vacuum annealing and before the surface analysis so it is difficult to discern changes that occurred during annealing from those that occurred during air exposure. The low quality of the vacuum introduces another factor which is discussed below.

Figure 2c shows an ESCA spectrum of the Cp 2p and O 1s peaks taken after annealing the sample in vacuum (10^{-4} Torr). The O/Cr atomic ratio is 2.2, which is lower than that obtained from either the as-prepared sample or the sample annealed in air. The O 1s peak is now broad and has a peak position of 531.0 eV. It appears to be composed of two peaks assigned as oxygen bonded as Cr_2O_3 and oxygen bonded as hydroxyl groups and adsorbed water. This can be observed clearly in Figure 4c. The high-resolution ESCA Cr 2p peaks shown in Figure 3c indicate that the Cr is primarily present as Cr_2O_3 but that some CrO_3 and metallic Cr are also present. Small amounts of Cr_2S_3 and CrO_2 may also be present. These data suggest that Cr_2O_3 and metallic Cr were formed during the vacuum annealing and that other oxides and hydroxides probably formed on the metallic Cr during the air exposure before the surface characterization studies were performed. This interpretation is also consistent with the depth profiling data described below.

All three Auger spectra shown in Figure 1 contain a significant C peak. The as-prepared sample yields the smallest C peak. ESCA C 1s spectra taken from the as-prepared surface, the air-annealed surface, and the vacuum-annealed surface are shown in Figure 5, spectra a–c, respectively. The C on the as-prepared sample predominantly consists of Cr carbide, some graphitic C and possibly a small amount of C bonded to O as carboxylic groups. After annealing in air or vacuum (10^{-4} Torr), the predominant form of C present is graphitic, but small shoulders due to Cr carbide and COOH appear to be present.

Figure 6a shows an AES spectrum taken after sputtering an as-prepared conventional Cr sample for 19 h. Large changes between this spectrum and the AES spectrum of Figure 1a are observed. The S and the C are reduced to trace quantities, an Ar peak appears near 220 eV, and the O peak is greatly reduced. The AES C peak shape is clearly indicative of carbide. The corresponding ESCA spectrum shown in Figure 7 agrees with the AES spectrum in that the O peak is now very small. The predominant form of the Cr is metallic, and a small shoulder most likely due to Cr_2O_3 is present.

An AES spectrum taken after sputtering (19 h) the sample annealed in 10^{-4}-Torr vacuum is shown in Figure 6b. Compared to Figure 6a, this spectrum contains large S, C, and O peaks. Compared to the AES spectrum shown in Figure 1c taken from the surface of the vacuum-annealed sample, it can be seen that the S peak essentially remains unchanged, an Ar peak due to sputtering appears, the C AES peak shape changes from graphitic to carbidic,

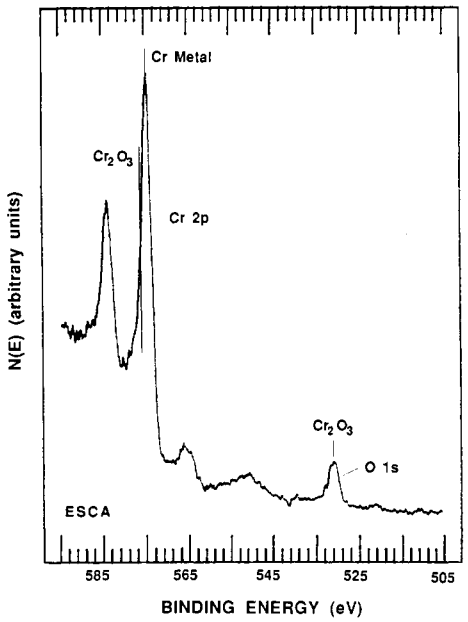

Figure 7. Cr 2p and O 1s ESCA spectrum taken from the as-prepared sample after ion sputtering for 19 h.

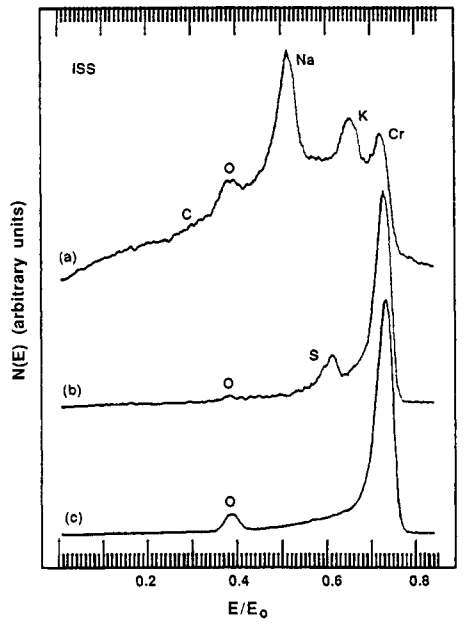

Figure 8. ISS spectra taken from (a) the as-prepared sample, (b) the same surface after annealing at 500 °C for 1 h in a 10^{-9}-Torr vacuum, and (c) the surface shown in (b) after ion sputtering for 1.5 h.

and the height of the O peak is greatly reduced. It is improbable that the low sputtering rates used in this study converted graphitic C into carbidic form. These differences are discussed further below with regard to the depth profiling results.

Ion scattering spectroscopy (ISS) is a very important surface analytical technique because it is sensitive to the outermost layer of atoms, whereas both AES and ESCA probe considerably more deeply. An ISS spectrum taken from the as-prepared surface is shown in Figure 8a. Peaks due to Cr, O, Na, and K are readily apparent in this spectrum. In ISS the cross section of the scattering event increases as the mass of the scattering atom increases. Although C has a very small ISS cross section, it appears that a feature due to C may be present at an E/E_0 of 0.28.

After characterizing the as-prepared sample, it was annealed in ultrahigh vacuum (10^{-9} Torr) at 500 °C for 1 h.

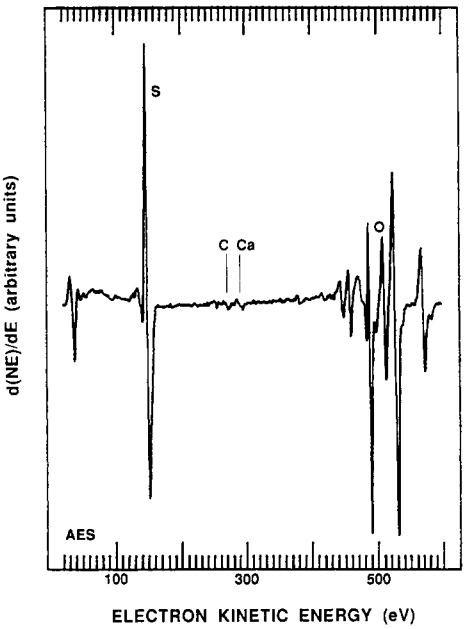

Figure 9. AES spectrum taken from the as-prepared sample after annealing in a 10^{-9}-Torr vacuum for 1 h at 500 °C.

An AES spectrum taken from this surface is shown in Figure 9, and the corresponding ISS spectrum is shown in Figure 8b. Comparing the AES spectrum taken after heating to that taken before heating (Figure 1a), the S peak is greatly increased and the O peak is greatly decreased but not eliminated. This demonstrates that S migrates to the near-surface region and that the O concentration in this region is decreased by migration of O into the bulk or by desorption. Furthermore, the K peak is eliminated by the annealing, and the C peak is greatly decreased. The ISS spectrum shown in Figure 8b is in agreement with these observations. After annealing (10^{-9} Torr) the outermost atomic layer contains Cr, S, and only a trace of O. The Na and K desorb probably as oxides during the annealing, the O migrates into the bulk, and S migrates from beneath the bulk into the outermost atomic layer. An ISS spectrum taken after a mild sputtering is shown in Figure 8c. The sputtering removes the S at the surface and exposes subsurface O. The ISS results obtained from the conventional Cr film correlate well with AES results obtained from ABCD films.[7]

The AES depth profiling results obtained from the as-prepared conventional Cr sample are shown in Figure 10. The atomic fractions of Cr, O, C, S, N, and Ar are plotted as functions of sputter time. The atomic ratios were obtained simply by measuring the various peak heights and using the sensitivity factors and standard procedure given in ref 11. Quantification of AES data is quite difficult in this case because the Cr and O peaks overlap somewhat, the various chemical states present have largely varying peak shapes, and the composition varies significantly with depth. Some of these factors pertaining to quantification of the O/Cr system have been discussed by Siconolfi and Frankenthal.[13] Therefore, it is reasonable to consider that the atomic percents shown in Figures 10–13 are only semiquantitative but that the variational trends in composition with depth and from one sample to another are meaningful. The atomic concentration data are reproducible, but the precision is not known. In these depth profiling

(13) Siconolfi, D. J.; Frankenthal, R. P. *Corros. Sci.* **1984**, *24*, 137.

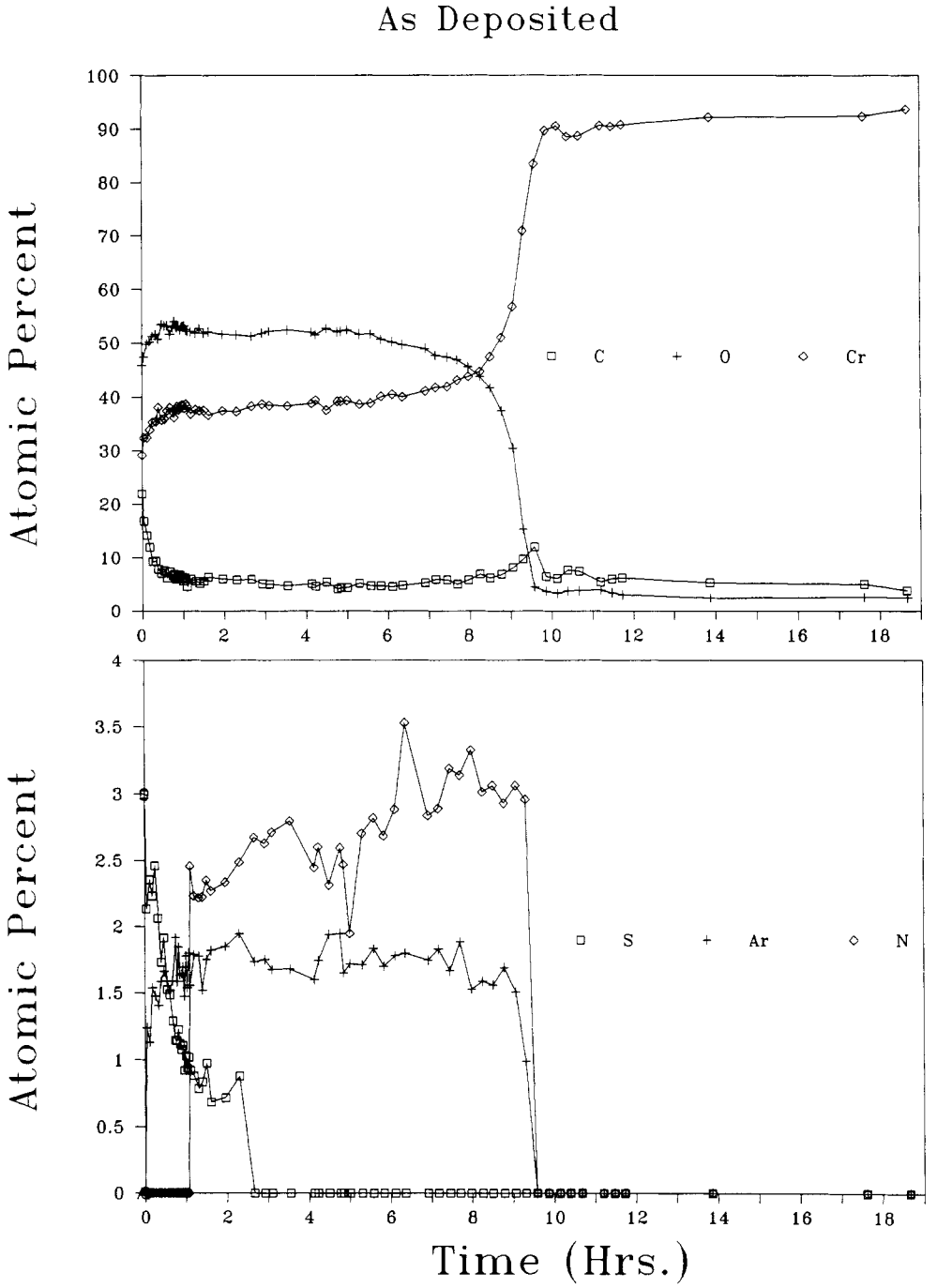

Figure 10. AES depth-profiling data obtained from the as-prepared conventional Cr surface.

experiments, the sputter rate is not known, and it probably varies from sample to sample and with depth for a given sample as the composition and hardness change. The data of Figure 10 show that an oxide layer is present above a metal-rich region. This is consistent with the AES and ESCA spectra shown in Figures 1a, 2a, 3a, 6a, and 7. The O/Cr atomic ratio is about 1.25, which suggests that the oxide layer contains some metallic Cr in agreement with the Cr 2p ESCA spectrum in Figure 3a. The O concentration decreases dramatically at the oxide/metal interface and remains small but constant at a value of about 2 at. % throughout the metallic region. The C concentration is fairly constant throughout the entire Cr film, but the surface concentration is nearly twice the bulk concentration. This is probably due to the adsorption of C-containing contaminants at the surface. A C concentration spike appears at the oxide/metal interface, but this is an artifact due to knock-on during the sputtering process. In knock-on a portion of the C moves into the solid rather than sputtering off the surface. The C that is knocked into the solid then accumulates at the interface rather than being knocked into the metallic layer, resulting in an artificially high C concentration at the interface. Most of the S lies near the surface at a small concentration and is sputtered away fairly rapidly. The fact that Ar imbeds only in the oxide layer and not the metallic layer is interesting. This implies that it imbeds in a defect structure and possibly in O vacancies which are not present in the metallic portion of the Cr film. N is present at about 3 at. % throughout the oxidic layer but is not present in the metallic layer, which suggests that N in the air provides the source for N in the film.

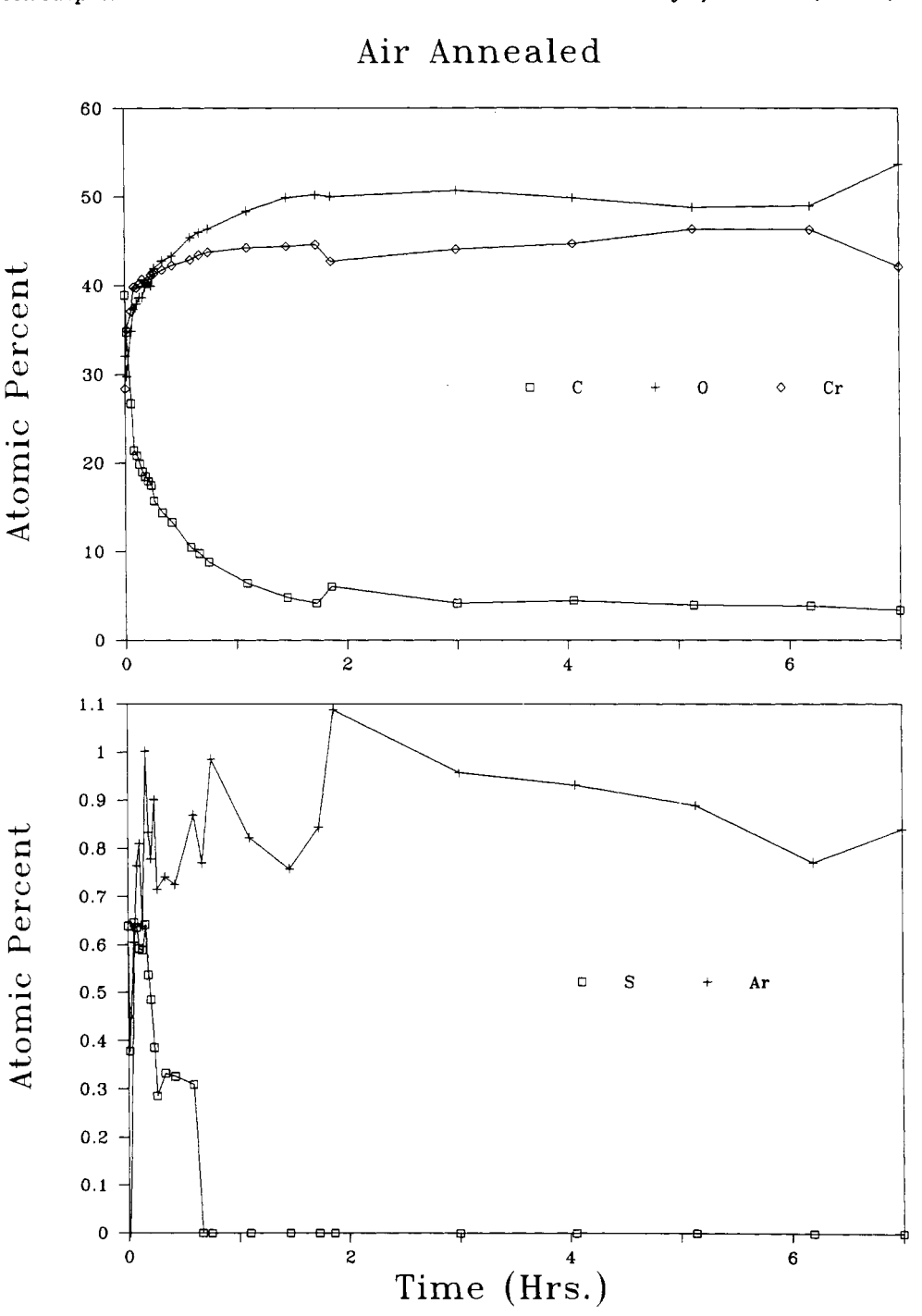

Figure 11. AES depth-profiling data obtained from the air-annealed (600 °C for 30 min) Cr surface.

AES depth profiling results taken from the air-annealed sample during a 7-h sputter period are shown in Figure 11. The O and Cr concentrations increase during the initial sputtering period as the C concentration declines sharply from 40 to about 4 at. %. A portion of the Cr is bonded as Cr_7C_3, and the rest is bonded as Cr_2O_3. This assertion is consistent with both the O/Cr and Cr/C atomic ratios in the depth profiling data and the ESCA Cr 2p spectrum presented in Figure 3b. Annealing the film in air decreases the O/Cr ratio as stated above. Only a very small amount of S remains in this film near the surface. This film was sputtered for a total of 16 h, and no oxide/metal interface is observed in the depth profiling data. This suggests that the overall O content of the film is increased by annealing in air. Most of the S migrates to the surface during air annealing and probably desorbs as SO_2.

The AES depth profiling results taken from the film after annealing in a 10^{-4}-Torr vacuum for 30 min at 600 °C are shown in Figure 12. It is clear that this process produces large changes in the compositional profiles (compare Figure 12 with Figure 10). It appears that much of the O in the oxide layer migrates into the more metallic portion of the film during the annealing, but no distinct oxide/metal interface is present after the vacuum annealing. It is possible that some of the O near the surface desorbs from the surface. This may explain the dip in O concentration just beneath the surface. The C content of this film is very high at an atomic fraction of about 0.25 throughout the bulk and a much higher concentration near

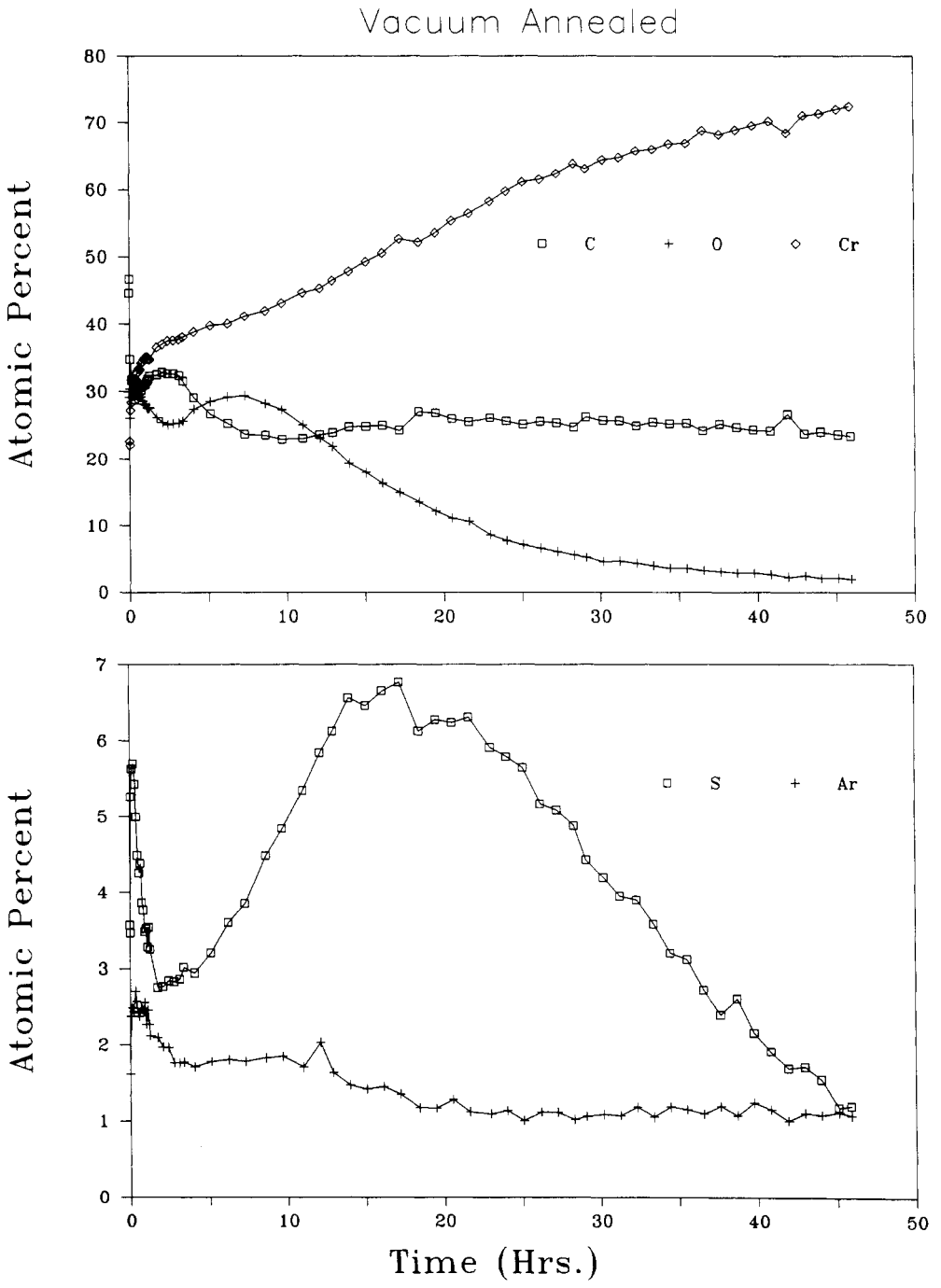

Figure 12. AES depth-profiling data obtained from the vacuum-annealed (10^{-4} Torr, 600 °C for 30 min) Cr surface.

the surface. The vacuum background of 10^{-4} Torr consisted of mostly hydrocarbons since the vacuum system was mechanically pumped. These hydrocarbons apparently are adsorbed on the Cr during the annealing period and migrate into the bulk of the film. It is most interesting that the AES C peak shape indicates that the C is carbidic throughout the whole film (see Figure 6b), but the ESCA spectrum shown in Figure 3c indicates that the C at the surface is primarily graphitic. These statements are consistent with the assertion that hydrocarbons adsorb at the surface and migrate into the bulk, forming a carbide. The S concentration is unusual in that a large dip appears just beneath the surface. It is possible that S near the surface reacts with oxygen in the background gas and desorbs and that S lying deeply beneath the surface migrates toward the surface, resulting in the second decrease in concentration after sputtering for 17 h. The Ar implants in this film throughout the entire sputtering period.

The depth profiling results obtained from a sample annealed in 10^{-9}-Torr vacuum for 1 h at 500 °C is shown in Figure 13. The vacuum background consisted mostly of hydrogen, water, and CO at very low partial pressures in this case. Essentially no change occurs after 0.8 h of sputtering, so only the profiles obtained during the first 2 h of sputtering are shown. During this treatment, the O in the oxide layer migrates to the surface and desorbs, leaving a metallic-rich Cr film. A very high O concentration of about 46 at. % is present at the surface, but this oxide layer is very thin, requiring only about 4 min to be sputtered away. After sputtering for about 0.8 h, the O concentration is reduced to about 6 at. % and remains nearly constant thereafter. The Cr concentration increases as the O concentration decreases, and it reaches a steady-state value of about 86 at. %. The C is fairly

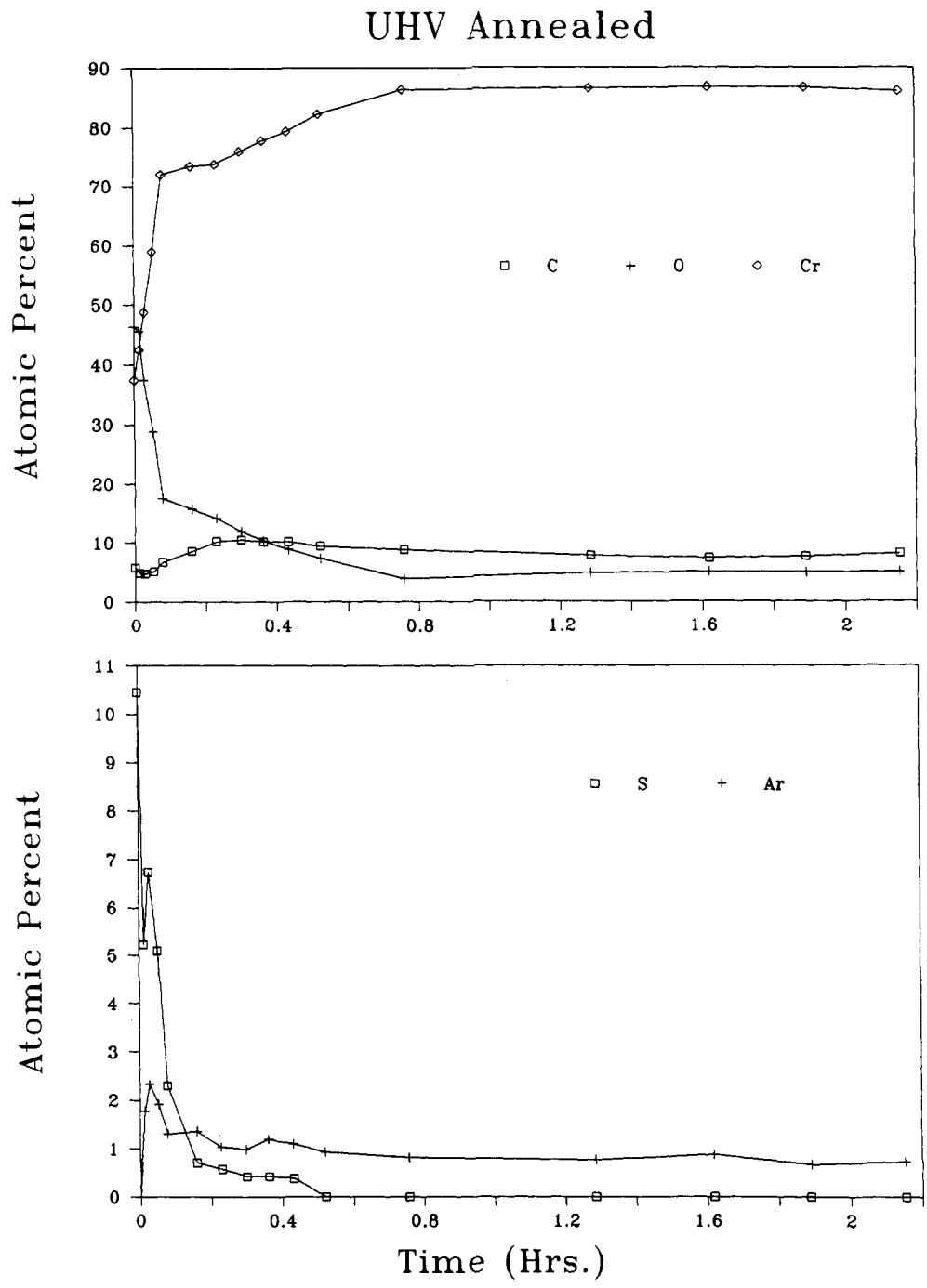

Figure 13. AES depth-profiling data obtained from the vacuum-annealed (10^{-9} Torr, 500 °C for 1 h) Cr surface.

uniformly distributed throughout this film at a concentration of about 8 at. %, which is similar to that contained in the as-prepared film. The C is carbidic in the UHV-annealed film. A large amount of S is present at the surface (see Figure 9), but its concentration quickly decreases to a trace quantity of <0.5 at. %.

Conclusion

AES, ESCA, ISS, and sputter-depth profiling have been used to characterize conventional Cr films. A comparison of the chemical composition and chemical states of species contained in conventional chromium films, air-annealed films, and vacuum-annealed films is presented. The as-prepared conventional Cr sample contains Cr, C, O, S, Ca, K, Cl, and Na. Hydrogen is probably present but is not observed with the techniques used in this study. The Cr in the near-surface region of an as-prepared film exists mostly as chromium oxides (CrO_3, CrO_2, and Cr_2O_3) and also as Cr_2S_3 and metallic Cr. The C is mostly of graphitic form. The oxygen is probably present mostly as hydroxyl groups and absorbed water. Below the oxide layer lies a metal-rich layer.

Annealing the sample in air at 600 °C causes most of the S to desorb from the surface probably as SO_2. The Cr is almost completely oxidized to Cr_2O_3, and the O content remains high throughout the entire film. The C segregates to the surface where it is present in graphitic form.

Annealing the sample at 600 °C in a 10^{-4}-Torr vacuum for 30 min causes O to both desorb from the film and migrate into the bulk of the film. A large amount of C is incorporated into the film by annealing in a hydro-

carbon-rich environment. This C is carbidic in nature.

Annealing the sample at 500 °C for 1 h in a 10^{-9}-Torr vacuum results in migration of the S and O to the near-surface region. The S lies in the outermost atomic layer with the O lying in the subsurface region. Most of the O desorbs, and the C and O concentrations are low throughout the bulk of the film.

Acknowledgment. We appreciate support of this research received from T. Miyasaka, President of OTEC Co., LTD.

Registry No. S, 7704-34-9; C, 7440-44-0; Cl_2, 7782-50-5; O_2, 7782-44-7; Ca, 7440-70-2; K, 7440-09-7; Na, 7440-23-5; Cr_2O_3, 1308-38-9; CrO_2, 12018-01-8; CrO_3, 1333-82-0; Cr_2S_3, 12018-22-3; Cr, 7440-47-3.

Deep Anisotropic Etching of Tapered Channels in (110)-Oriented Silicon

Edward S. Kolesar, Jr.,* and Michael W. Carver

Air Force Institute of Technology, Department of Electrical and Computer Engineering, Wright-Patterson Air Force Base, Dayton, Ohio 45433-6583

Received June 20, 1989

A 50 wt % potassium hydroxide and deionized water anisotropic etchant was utilized to isothermally (85 °C) etch a staggered array of deep (290 μm), 5-μm wide, closely spaced (20.4 μm), smooth-walled, tapered channels in (110)-oriented silicon wafers. A quantitative relationship that specifies the channel length as a function of the channel width and depth is developed. A buffered hydrofluoric acid isotropic etchant was employed to sharply point the top edges of the channel walls.

Introduction

Single-crystal silicon has revolutionized technology during the past 20 years comparable to that attributed to steel in the midst of the industrial revolution. The most prominent technological contribution of silicon has been the emergence of the integrated circuit (IC) electronics industry.[1] In addition to its favorable and comprehensively documented electrical properties, silicon possesses exemplary mechanical and thermal characteristics. Silicon commands a substantially higher stiffness-to-weight ratio compared to most common materials, including steel and titanium.[2] In addition, silicon is a good conductor of heat, comparable with aluminum at room temperature; and similar to diamond, its thermal conductivity increases with decreasing temperature.[2] As a result of the mechanical characteristics being coupled with the precise IC microfabrication technology that was developed for patterning and etching silicon, a host of novel microelectronic, electrochemical, electromechanical, and micromechanical devices and components have recently emerged. Several extensive reviews of the basic processes and structures are available in the literature.[2-9] It is now common practice to refer to the fabrication of sophisticated three-dimensional micromechanical structures from silicon as micromachining.[2-5]

The anisotropic etching mechanism of silicon has been attributed to the crystallographic properties of the various planes, and it has been experimentally verified to be particularly sensitive to the atomic packing density. Accordingly, the relative etch rate decreases as the atomic packing density increases. Since the packing density of silicon atoms is substantially greater in the ⟨111⟩ direction compared to the ⟨100⟩ or ⟨110⟩ directions, the {111} planes etch much slower compared to either the {100} or {110} planes.[6-9]

There are three common anisotropic etchants for (100)- and (110)-oriented silicon. The most intensively studied etchant is the potassium hydroxide–water (KOH) system. For example, a 50 wt % mixture of each component at 85 °C exhibits an etch rate of 1.43 μm/min for the (100) plane, 0.6 μm/min for the (110) plane, and 0.007 μm/min for the (111) plane. Correspondingly, the differential etch rates are approximately 200/1 for the (100)/(111) planes and 86/1 for the (110)/(111) planes.[5,10-15] On the other hand, the ethylenediamine–pyrocatechol–water (EDP) etchant (typically, 750 mL–120 g–240 mL at 115 °C) manifests an etch rate of 1.25 μm/min for the (100) plane and a 35/1 differential etch rate for the (100)/(111) planes.[16-26] Finally and less thoroughly investigated is the hydrazine–

(1) Petersen, K. E. *Proc. Int. Elec. Dev. Mtg. (IEDM)*; Washington, D.C., Dec 1-4, 1985; Vol. 2, session 1.1, pp 2-7.
(2) Institute of Physics; Instrument Science and Technology Group; Short Meeting Series, No. 3, *Silicon Based Sensors*; London, Dec 8, 1986.
(3) Delapierre, G. *Sens. Acutators* **1989**, *17*, 123-138.
(4) Shoji, S.; Esashi, M.; Micromachining for Chemical Sensors. *Chemical Sensor Technology*; Seiyama, T., Ed.; Elsevier: New York, 1988; Vol. 1, pp 179-193.
(5) Fung, C. D., Cheung, P. W., Ho, W. H., Fleming, D. G., Eds.; *Micromachining and Micropackaging of Transducers*; Elsevier: New York, 1985.
(6) Petersen, K. E. *Proc. IEEE* **1982**, *70*, 420-457.
(7) Bassous, E. *IEEE Trans. Electron. Dev.* **1978**, *ED-25*, 1178-1185.
(8) Bean, K. E. *IEEE Trans. Electron. Dev.* **1978**, *ED-25*, 1185-1193.
(9) Ammar, E. S.; Rodgers, T. J. *IEEE Trans. Electron. Dev.* **1988**, ED-27, 907-914.
(10) Stoller, A. I. *RCA Rev.* **1970**, *31*, 271-275.
(11) Price, J. B. Anisotropic Etching of Silicon with Potassium Hydroxide-Water-Isopropyl Alcohol. *Semiconductor Silicon*; Huff, H. R., Burgess, R. R., Eds.; The Electrochemical Society Softbound Symposium Series: Princeton: NJ, 1973; p 339.
(12) Kendall, D. L. *Ann. Rev. Mater. Sci.* **1979**, *9*, 373.
(13) Weirauch, D. F. *J. Appl. Phys.* **1975**, *46*, 1478.
(14) Allen, D. M.; Routledge, I. A. *IEE Proc. Part 1* **1983**, *130*, 49-56.
(15) Linden, Y.; Tenerz, L.; Tiren, J.; Hok, B. *Sens. Actuators* **1989**, *16*, 67-82.
(16) Kaminsky, G. *J. Vac. Sci. Technol., B* **1985**, *3*, 1015-1024.
(17) Greenwood, J. C. *J. Electrochem. Soc.* **1969**, *116*, 1325.
(18) Bohg, A. *J. Electrochem. Soc.* **1971**, *118*, 401.
(19) Reisman, A.; Berkinblit, M.; Chan, S. A.; Kaufman, F. B.; Green, D. C. *J. Electrochem. Soc.* **1979**, *126*, 1406.
(20) Finne, R. M.; Klien, D. L. *J. Electrochem. Soc.* **1967**, *114*, 965-970.